



In vitro and *in vivo* evaluation of microneedles coated with electrosprayed micro/nanoparticles for medical skin treatments

Serdar Tort^{a,b} , Necibe Basaran Mutlu Agardan^b , Daewoo Han^a  and Andrew J. Steckl^a 

^aNanoelectronics Laboratory, Department of Electrical Engineering and Computer Science, University of Cincinnati, Cincinnati, OH, USA; ^bDepartment of Pharmaceutical Technology, Faculty of Pharmacy, Gazi University, Ankara, Turkey

ABSTRACT

Aim: Microneedles (MNs) create micropunctures and deliver drugs or nutrients deep into skin layer. We demonstrated that MNs, coated with electrosprayed nanoparticles loaded with functional molecules, are useful for transdermal delivery.

Methods: Electro spraying was utilised to generate drug-loaded nanoparticles and to create uniform coating on MNs. Process parameters and release kinetics were evaluated *in vitro*. The *in vivo* efficacy of insulin-coated MNs was investigated using diabetic rats.

Results: Electro sprayed micro/nanoparticles loaded with dye or insulin were coated on MNs with particle size of 515 ± 286 and 522 ± 261 nm, respectively. Optimally coated MNs resulted in $>70\%$ transfer rate into porcine skins. Insulin-coated MNs were applied to diabetic rats resulting in reduction of blood glucose levels fluctuations, compared to subcutaneous injections.

Conclusions: Electro spraying is shown to be an effective method to coat MNs with drug-loaded nanoparticles. Coated MNs provide a promising platform for cosmetic, drug and protein delivery applications.

ARTICLE HISTORY

Received 16 April 2020

Accepted 10 August 2020

KEYWORDS

Electro spraying; electrohydrodynamic atomisation; microneedle; dermaroller; skin; drug delivery

1. Introduction

Microneedles (MNs) are one of the best options for painless drug delivery via skin penetration because they have several advantages over conventional hypodermic needles (Gill and Prausnitz 2007), such as minimal invasiveness, reduced infection risk, ease of administration, reduced skin irritation at and near the injection site. Another skin-based delivery approach is the transdermal drug delivery (TDD) wherein drugs loaded in patches placed on the skin diffuse through the top skin surface (stratum corneum) to introduce the drug molecules into the blood stream. The patches are non-invasive approach and quite easy to use (Nejad *et al.* 2018). However, because TDD uses diffusion through the skin layers, it requires a relatively large dose to be effective and it is very challenging to deliver advanced large drug molecules.

Microneedles do present some potential issues, such as local inflammation on sensitive and allergic skin, and the possibility of broken MN tips that may be left under the skin. Broken MN tip issue can be avoided by using stainless steel MNs instead of silicon MNs, and local inflammation can be minimised by

using smaller MNs (Escobar-Chávez *et al.* 2011). The height of the MNs affects the level of pain stimulation, related to the penetration depth into the stratum corneum (10–20 μm), the epidermis (~ 100 – 200 μm) and the dermis (~ 1 – 2 mm). MNs with height of 1.5–2 mm are routinely used for treating acne and scars, while shorter MNs with height of 0.5–1.0 mm are used for treating aging skin and wrinkles (Singh and Yadav 2016, Iriarte *et al.* 2017). If epidermal cells are targeted, relatively short MNs (200–300 μm) are suitable. For other medical treatments, longer MNs are appropriate. Usually the treatment process is painless with MNs up to 0.5 mm height, but it is also a function of the epidermis thickness of the individual receiving treatments (Singh and Yadav 2016). A simple but limited approach is to use an array of solid MNs to create small holes on stratum corneum of the skin through which drugs from a topical formulation can diffuse into the skin more efficiently than from a transdermal patch. More complex approaches, such as using hollow MNs for drug injection and dissolvable MNs for the patient's convenience as an easy one-step process, have been reported to deliver insulin, heparin, anti-cancer agents, gene therapy vectors and vaccines

through the skin (Escobar-Chávez *et al.* 2011, Kim *et al.* 2012, Baek *et al.* 2017).

Drug-coated MNs are a promising delivery system for drug molecules that cannot be administered orally due to enzymatic degradation or poor absorption. Tools with solid MNs (stainless steel or titanium), currently used for creating punctures to increase skin permeability, can be coated with active ingredients using various methods, such as dip-coating, gas-jet drying, spray coating, electro-spraying and 3D printing. The simplest MN coating technique is dip coating, wherein solid MNs are immersed into a drug-containing solution and then dried. One of the challenges for this method is non-uniform and imprecise coating thickness (Chen *et al.* 2017). Chen *et al.* (2009) have used a gas-jet drying method to produce ovalbumin-coated MNs. In this method, a small volume of solution was cast on a whole MN patch. Then, a pressure gas jet quickly dried the coating layer while the excess coating solution is removed, avoiding a thick coating on the base between MNs. However, the coating on the base is not completely prevented (Ingrole and Gill 2019). The ink-jet printing process exhibits good control with minimum waste of coating material and good reproducibility (Pere *et al.* 2018). However, some researchers reported it is challenging to provide mass production capabilities due to time consuming process to coat the large number of MNs (Chen *et al.* 2017). Another interesting approach is using 3D printing methods, such as 3D ink-jet printing, fused deposition modelling (FDM), stereolithography (SLA) and selective laser sintering (SLS). SLA method uses consecutive layer-wise photopolymerization of UV-sensitive polymers and provides very good quality of microstructures. Economidou *et al.* (2019) successfully combined 3D printing and ink-jet printing methods for fabrication of insulin-coated MNs. They produced MN arrays via SLA method and coated MNs with insulin using an ink-jet printer.

The spray coating process of MNs consists of three steps: atomisation generating fine solution droplets; deposition of droplets onto the surface of MNs; coalescence forming a continuous film coating (McGrath *et al.* 2011, Vrdoljak *et al.* 2012, Haj-Ahmad *et al.* 2015). This coating process is sensitive to solution properties (surface tension, viscosity and density) and spray conditions (spray velocity and spray density). Electrohydrodynamic atomisation (*aka* electro-spraying) is another spraying approach based on electrostatic forces for producing micro/nanoparticles. Electro-spraying and electro-spinning have similar principles and instrumental set-ups (Han and Steckl 2017, Han *et al.* 2017). In this method, an electrical field charges the polymer droplets and

produces a jet through a capillary nozzle (Jaworek 2007, Jaworek and Sobczyk 2008). The resulting micro/nanoparticles are subsequently collected on a ground electrode positioned under the nozzle tip. The advantages of electro-spraying method compared to other methods are: (a) targeting conductive materials for the electro-sprayed charged droplets; (b) controlling the shape and dimensions of electro-sprayed nanoparticles; (c) providing immediate or sustained release of transferred nanoparticles using hydrophilic or hydrophobic carriers, respectively (Guo *et al.* 2015). Furthermore, core-shell micro/nanoparticles can be produced using two solutions being fed into a coaxial nozzle. The process parameters (applied voltage, solution flow rate, electrode separation) affect the particle size, distribution, shape and surface morphology. If the process is not optimised for electro-spraying, nanofibers can be produced instead of nanoparticles, which cause a bridging issue between MNs.

Type 1 diabetes mellitus therapy requires insulin injections in order to control blood glucose levels. Multiple daily injections of insulin mostly result in pain and patient discomfort (Aronson 2012). Therefore, various approaches explored to achieve non-invasive insulin delivery via oral, transdermal, buccal or nasal routes (Shah *et al.* 2016). Recent studies on MNs showed that MNs could provide effective and painless insulin delivery hence improves patient compliance. Pettis *et al.* (2011) suggested that intradermal insulin injection with MNs (1.25–1.75 mm) provided safe and well tolerated therapy compared to subcutaneous injection. In another study, Gupta *et al.* (2009) reported that hollow glass MNs were effective in reducing blood glucose levels without pain and adverse effect in human volunteers.

Among other examples, the electro-spraying process has been utilised to produce natural or synthetic/semi-synthetic micro/nanoparticles incorporating various drug molecules, such as insulin, folic acid and anti-microbial agent (Haj-Ahmad *et al.* 2015). Although electro-sprayed micro/nanoparticles can provide either sustained release or immediate release drug profiles, very limited studies have been reported on coating of MN via the electro-spraying method. Khan *et al.* (2014) coated stainless steel MN with fluorescein dye/polyvinylpyrrolidone (PVP) via the electro-spraying method. They reported that fibres were also deposited along with particles on the MNs during the electro-spraying process. In our study, we investigated the coating of dermarollers containing 540 stainless steel MNs of two different heights and diameters (0.25 mm/80 μ m and 2 mm/300 μ m) with a water-soluble polymer and dye (Figure 1(a)). At these dimensions, the MNs penetrate

the stratum corneum barrier and reach the epidermis/dermis (Figure 1(b)). Nanoparticles coating the MNs can dissolve into the skin interstitial fluid and diffuse to the adjacent microcapillary beds for efficient absorption into the systemic circulation (Peters *et al.* 2012). The effects of process parameters (electric field, electro spraying time) and solution parameters (molecular weight, solvent properties) on the coating process have been evaluated. Water-soluble Keyacid Red dye was used as a model molecule and release studies were conducted. The diffusion properties of coated MNs were investigated using both gelatine gel and porcine skin. To verify the *in vivo* efficacy, dermarollers with MNs were coated with insulin as a model protein and applied to diabetic rats. The blood glucose level was evaluated for 6 h and compared with the traditional subcutaneous injection treatment. Dermarollers coated with electro sprayed nanoparticles successfully transferred the dye and insulin directly into the skin. Hence, this approach is proposed as an

innovative and user-friendly method for the effective delivery of cosmetic ingredients, nutrients, drugs or proteins.

2. Materials and methods

2.1. Materials

Low and high molecular weight polyethylene oxide (PEO HM, Mn 1000 kDa; PEO LM, Mn 100 kDa) and gelatine (from bovine skin, Type B) were purchased from Sigma Aldrich (St. Louis, MO). Water-soluble Keyacid Red XB (KAR) dye was used as a model ingredient. Ethanol was purchased from Fisher Scientific (Pittsburgh, PA). Human insulin solution (Humulin R, 100 IU/mL) was purchased from Eli Lilly and Company (Indianapolis, IN).

2.2. Electro spraying process

To determine the solution parameters on electro spraying process, PEO with two different molecular weights (PEO LM, PEO HM) and two different solvents (deionised water (DI), ethanol) were used and five different electro spraying solutions were prepared (Table 1). These solutions were electro sprayed on two different dermarollers with the MN height of 0.25 or 2 mm at different applied voltages.

Electro spraying solutions containing PEO LM were prepared at a concentration of 10% w/v, while solutions containing PEO HM were prepared at a concentration of 1% w/v. For preparing F1–F3, the PEO solution was homogenised using a rotating stirrer for 24 h at room temperature. Because electro spraying of ethanol-based PEO HM solution (1% w/v) was not possible due to its high viscosity, ethanol-based PEO electro spraying studies were carried out only with PEO LM (F1). For further studies, 1% w/v KAR dye was added to water-based PEO LM solution (F4) and homogenised until all materials are fully dissolved. In order to avoid unexpected dripping of the polymer solution onto the dermaroller during electro spraying, the dermaroller was placed at the corner of the collector plate instead of the centre location directly under the

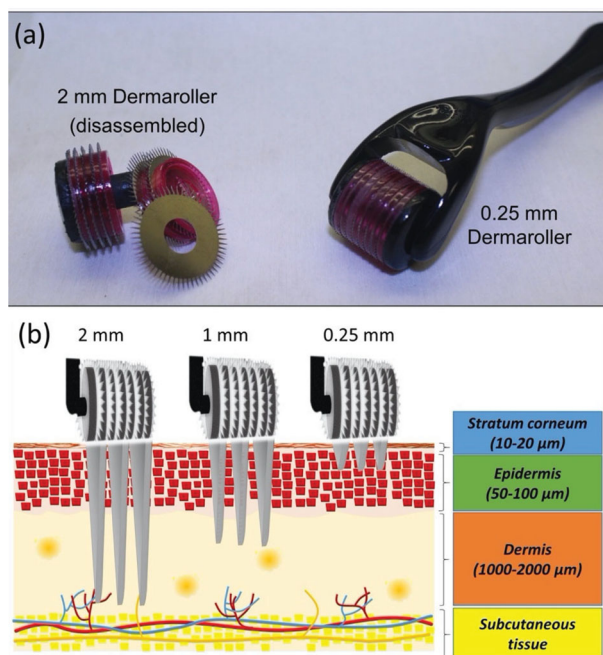


Figure 1. Application of microneedle containing dermarollers: (a) photographs of dermarollers with the MN height of 2 mm (disassembled) and 0.25 mm (assembled); (b) schematic illustration of dermaroller application to the skin.

Table 1. Compositions of different electro spraying solutions.

Formulation code	Polymer	Solvent	Polymer concentration (% w/v)	KAR dye concentration (% w/v)	Insulin concentration (IU/mL)
F1	PEO LM	Ethanol	10	–	–
F2	PEO LM	DI	10	–	–
F3	PEO HM	DI	1	–	–
F4	PEO LM	DI	10	1	–
F5	PEO LM	DI	10	–	100

DI: deionised water; KAR: Keyacid red; PEO LM: low molecular weight polyethylene oxide; PEO HM: high molecular weight polyethylene oxide.

needle tip. To evaluate the effect of applied voltage on electro spraying process, the voltage was varied between 14–18 kV for F2 and F3 formulation and 16–20 kV for F1 formulation. The distance and flow rate parameters were kept constant at 17 cm and 0.1 ml/h, respectively. After optimising electro spraying process parameters, the F4 formulation was electro sprayed at voltages of 16 and 18 kV on 0.25 and 2 mm MNs, respectively. For *in vivo* studies, 10% w/v PEO LM was added to insulin solution (F5 formulation) and mixed gently at room temperature. This solution was electro sprayed on two different dermarollers with the MN height of 1 and 2 mm under the following conditions: 18 kV voltage, nozzle to collector distance of 17 cm, and solution flow rate of 0.5 ml/h. Process time was kept at 30 and 15 min for 1 and 2 mm dermarollers, respectively. The loaded insulin amount was determined spectrophotometrically at 272 nm using BioSpec-nano instrument (Shimadzu, Japan) by a validated method (Yilmaz and Kadioglu 2012).

2.3. Dye loading and release studies

The effect of electro spraying time on the coating process was evaluated. After electro spraying for different time spans, coated dermarollers were immersed in DI to dissolve all electro sprayed nanoparticles and the optical density of solution was measured to obtain the total amount of coated dye on dermarollers at room temperature. Dye and insulin release studies from dermarollers were also carried out in DI and phosphate buffer solution (PBS, pH 7.4) at 37 °C, respectively. For this purpose, MNs were completely immersed in DI or PBS and sample solutions were taken for spectrophotometric measurements at predetermined times. All measurements were performed in triplicate.

2.4. Studies on gelatine gel and porcine skin

Although the majority of electro sprayed nanoparticles are deposited on the metallic MNs, some undesirable deposition also occurred on the dermaroller base, especially for the relatively short MNs of 0.25 mm. Therefore, dermarollers with 2 mm MNs were used for both gelatine gel and porcine skin studies. Clear gel plates prepared by dissolving 5% w/v gelatine in hot water were utilised to observe the cross-sectional diffusion of transferred dye from MNs (Ullah *et al.* 2018). Porcine skin was used for *ex vivo* studies to evaluate the amount of drug delivered into the skin. PEO/KAR nanoparticle-coated dermaroller was applied to pieces of porcine skin and then the dermaroller was

immersed in DI for measurement of the remaining nanoparticles on MNs (Ma and Gill 2014). To measure the residual nanoparticles on the skin surface, small wipes pre-soaked in DI were gently rubbed on the skin to collect the dye left on the skin surface. Then the wipe was placed back into the DI beaker to dissolve all collected materials from the skin surface, and subsequently used for optical quantification measurements. Finally, the amount of nanoparticles transferred into the skin layer was calculated by subtracting the combined amount of dye remaining on the needles and on the skin surface from the total dye amount of electro sprayed nanoparticles on MNs (Ma and Gill 2014).

2.5. *In vivo* studies

The animal study was approved by the Ethics Committee of Gazi University (Approval number: G.U.ET-20.021). Wistar Albino rats that weighed 300–350 g were used in the study. The animals were maintained under standard laboratory conditions throughout the study with a 12-h light:12-h dark cycle, at a temperature of 25 ± 2 °C. Diabetes was induced by a single intraperitoneal injection of streptozotocin (STZ) (60 mg/kg). STZ was dissolved in freshly prepared 0.01 M citrate buffer pH 4.5 just before the injection. Diabetes was confirmed 5 days later by evaluating blood glucose levels from tail vein blood samples using a glucose meter. Rats having fasted blood glucose levels of 300 mg/dL or higher were considered diabetic (Wang *et al.* 2012, Bulboacă *et al.* 2019).

The animals were randomly divided into four groups: control (no treatment applied), 1 mm MN (0.3 IU insulin), 2 mm MN (0.3 IU insulin) and subcutaneous (0.3 IU insulin). The dorsal part of each rat was shaved before the experiments with an animal hair clipper. The animals received unrestricted access to food (standard pellets) and water during the experiment day and fasted for 6 h throughout the experiment. Insulin-coated MNs were rolled on the skin slowly for 1 min to provide insulin release from MNs. Blood samples were collected from the tail vein at predetermined time intervals and measured blood glucose levels using a glucose meter.

3. Results and discussion

MNs can be fabricated using a variety of materials, including silicon, metal, ceramic, silica glass and polymers (Waghule *et al.* 2019). The metallic MN dermaroller provides a suitable condition for electro spraying

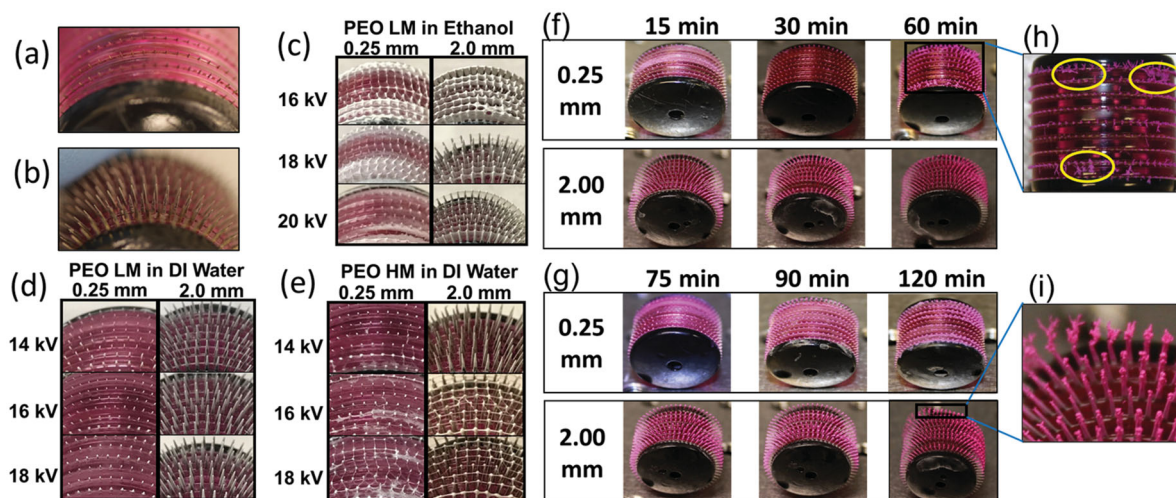


Figure 2. Effect of electrospaying process parameters on MN deposition: uncoated microneedles with heights of (a) 0.25 mm and (b) 2 mm. Electrospaying deposition of nanoparticles/nanofibers on dermarollers at different applied voltages using different polymeric solutions: (c) PEO LM in ethanol solution; (d) PEO LM in DI water solution; (e) PEO HM in DI water solution. Effect of electrospaying process time: (f, g) deposition of nanoparticles at different process times; (h) basement deposition of electrospayed particles; (i) dendrimer-like accumulation of nanoparticles on tips of MNs.

because the metallic MNs can be electrically grounded, attracting highly charged electrospayed aerosol to the MNs (Figure 1(a)). In this study, we have successfully deposited electrospayed nanoparticles on the MN array with different heights (Figure 2(a,b)). When the dermaroller is applied on the skin, rapid transfer of the micro/nanoparticles from the coated MNs should occur without the need for repeating applications. PEO is a biocompatible, safe, inert and generally non-immunogenic water-soluble polymer chosen for this study (Shiraishi and Yokoyama 2019). Many drug delivery systems, such as mucoadhesive, ocular, and injectable vehicles, are prepared with PEO in different molecular weights (Dhawan *et al.* 2005). In general, increasing the PEO molecular weight results in a slower release of incorporated drug molecules (Apicella *et al.* 1993). In this study, the electrospaying process using water-based polymer solutions was found to be more efficient than ethanol-based solutions. During electrospaying of ethanol-based PEO LM solutions, some fibre deposition over the MNs was observed at all voltages, leading to the bridging behaviour between MNs (Figure 2(c)). No fibre deposition occurred during electrospaying of PEO LM in water-based solutions at same voltage values (Figure 2(d)), while some fibres can be obtained using water-based PEO HM solution at relatively high voltages (Figure 2(e)). Because ethanol has lower surface tension and higher vapour pressure than water, some fibres were produced during electrospaying process with ethanol-based PEO solution. Also, increasing the

molecular weight caused additional chain entanglements within the polymer jet, leading to high probability of fibre formation. Electrospaying process with PEO LM in water-based solutions was successfully obtained at 18 kV for both 0.25 and 2 mm MNs (Figure 2(d)). Lower applied voltage caused more nanofiber deposition on MNs for F1 formulation compared to higher voltage values (Figure 2(c)). While nanofiber formation was not observed for F2 formulation at low voltage values, more particles were collected on MNs at the highest applied voltage (Figure 2(d)). Therefore, dye-loaded PEO LM water-based solution (F4 formulation) was electrospayed at the higher applied voltage of 18 kV.

Precise dose control and content uniformity are major challenges for conventional MN coating processes, such as dip coating, because of inconsistent coating on MNs (Chen *et al.* 2015). Uniformity of active pharmaceutical ingredient (API) is important as it will impact drug dissolution, absorption, bioavailability and onset of clinical effect (Alyami *et al.* 2017). Figure 2 also shows the effects of electrospaying process time on particle deposition. Increased electrospaying process time beyond ~1 h caused dendrimer-like branching of nanoparticles on the MN tip (Figure 2(f,g)) instead of deposition on the basement of dermaroller. Deposition for 60 min on 0.25 mm MNs resulted in some electrospayed nanoparticles being attached to the dermaroller base (Figure 2(h)). For the 2 mm MNs, with larger surface area, fewer nanoparticles were found deposited on the dermaroller base and

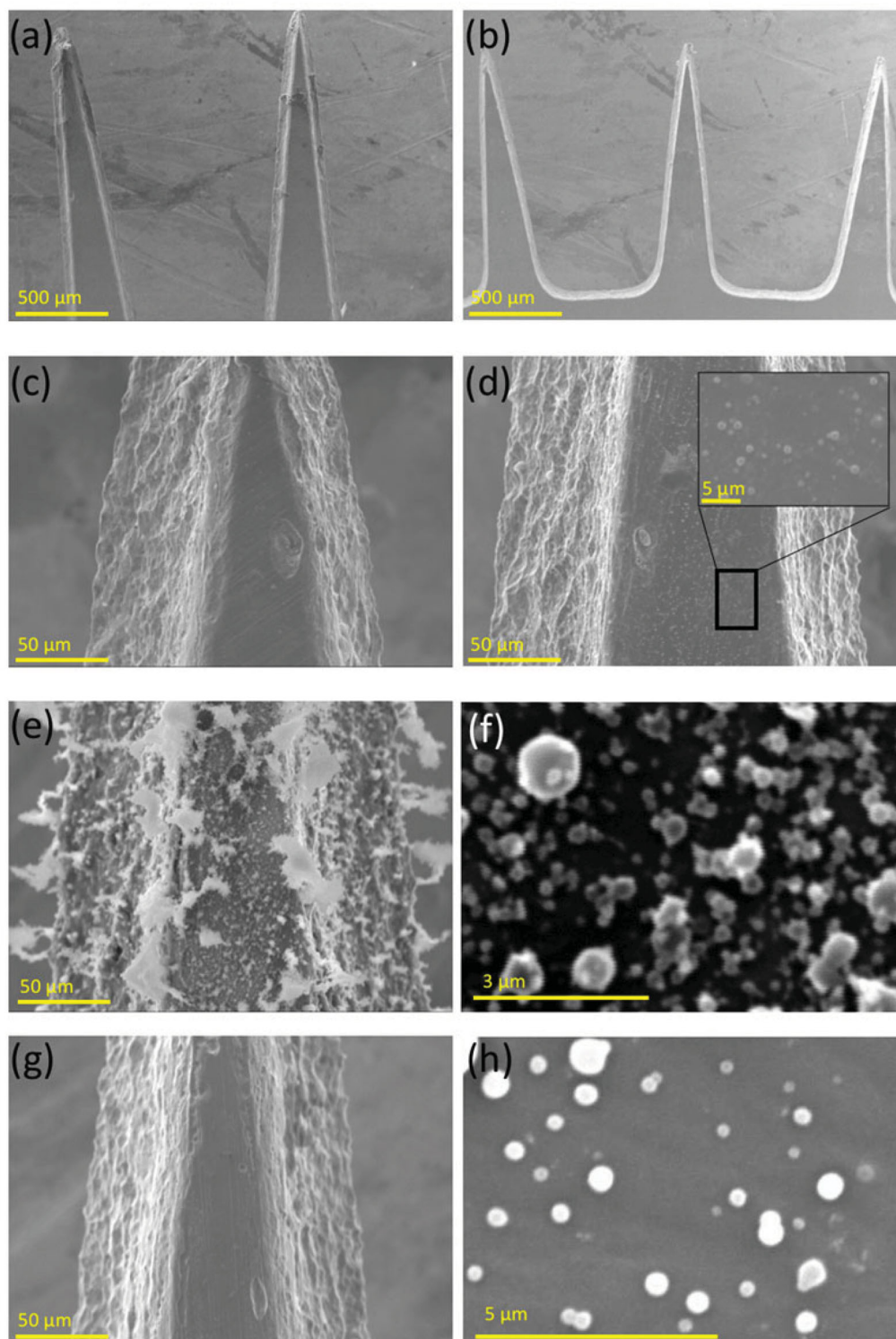


Figure 3. SEM photographs of microneedles: (a) uncoated 2 mm MNs; (b) uncoated 0.25 mm MNs; (c) uncoated 2 mm MN; (d) 3 min electrospayed 2 mm MN; insert shows electrospayed nanoparticles on MN surface; (e) 30 min electrospayed 2 mm MN; (f) electrospayed PEO-dye nanoparticles; (g) 2 mm MN surface after one-time application on porcine skin; (h) electrospayed PEO-insulin nanoparticles.

dendrimer-like branch growth became prevalent after ~ 120 min of electrospaying (Figure 2(i)). The base substrate of the MN array should remain uncoated to achieve higher delivery efficiencies (Ingrole and Gill

2019). Since only MNs penetrate the skin, any drug coated away from the MN is undeliverable and contributes towards an inefficient delivery process. The electrospaying method can provide uniform coating

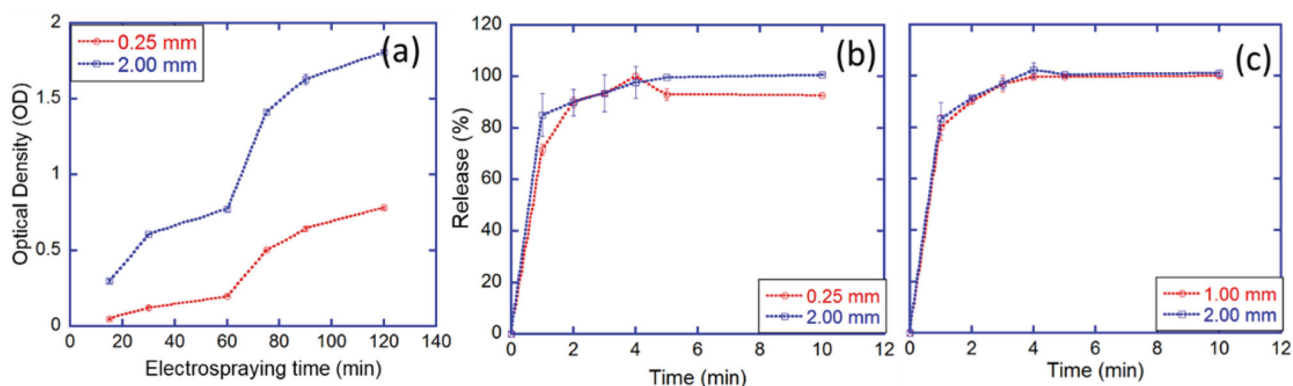


Figure 4. Loading capacity and release kinetics of electrospayed PEO nanoparticles (loaded either with KAR dye or insulin) on microneedle dermarollers: (a) total amount deposited on dermarollers as a function of electrospaying time, as determined by optical density (O.D.) measurement; (b) dye release kinetics from dermarollers; (c) insulin release kinetics from dermarollers (mean \pm SD) ($n = 3$).

on MNs with minimal deposition on the base of the dermarollers. Therefore, medical grade stainless steel or titanium MNs are good candidates for use with the electrospaying process (Figure 3). The distances between needle tips were 1200 and 1000 μm for the 2 and 0.25 mm MNs, respectively. Electrospayed micro/nano dye and insulin particles were coated on MNs with particle size of 515 ± 286 and 522 ± 261 nm, respectively (Figure 3(f,h)). Both PEO-dye and PEO-insulin particles exhibited spherical morphology, without fibre formation. Interestingly, some nanoparticles were deposited on previously deposited nanoparticles in Figure 3(f). This nanoparticle-on-nanoparticle deposition eventually forms nanoparticle branches as electrospaying deposition continues, shown in Figure 3(e).

Dye loading on the MN surface reaches a maximum after 60 min, beyond which particles are not coated on the MN surface but accumulate onto each other, forming dendrimer-like branches. The amount of dye particles deposited on both 0.25 and 2 mm MN dermarollers is shown in Figure 4(a) as a function of electrospaying time. As expected, increasing the electrospaying time increased the total dye amount on the MNs, with a greater dye amount being released from the 2 versus the 0.25 mm MN dermaroller. Interestingly, after 60 min the coated dye amount increased dramatically in both cases. As shown in Figure 3(d), electrospayed particles deposited first on the MN surface. After the MN surface is mostly coated, additional particles accumulate onto previously attached particles creating dendrimer-like branches (Figure 3(e)). This in effect increases the surface area, leading to increased particle deposition.

Yu *et al.* (2011) reported that electrospayed keto-profen-PVP nanoparticles showed more than 90% drug release within 60 s due to the high surface area

of nanoparticles and tremendous wettability of PVP. Li *et al.* (2018) coated MNs with colour-dyed polystyrene (PS) nanoparticles and PVP by dip-coating method. The complete release of dye from these MNs occurred within one half-minute. Similar to PVP, PEO is a biodegradable hydrophilic polymer and has the ability to increase the drug release rate (Hamoudi-Ben Yelles *et al.* 2017, Bass *et al.* 2018). In our study, dye loaded-PEO nanoparticles released $\sim 80\%$ of dye in 60 s and, as expected, there was no noticeable difference between the release profiles from the two dermarollers, as shown in Figure 4(b). Similarly, insulin release from 1.00 and 2.00 mm MNs was very rapid. More than 80% of the insulin released in 1 min for both MNs (Figure 4(c)). Anderson *et al.* (2016) prepared films with low molecular weight PEO (100 kDa) and reported that $\sim 80\%$ of drug released between 1 and 4 min. Our findings are in accordance with the study of Pere *et al.* (2018) in which they showed the rapid insulin release (63–69% in 2 min) from insulin coated MNs using Franz diffusion studies. The rapid release of insulin was related to the high hydration rates of coating material similar to PEO.

An initial indication of the insertion capability of coated MNs was obtained using gelatine gels. Gelatine gel is optically transparent with a similar composition to skin tissue and can be used for drug delivery evaluation of MNs *in vitro* (Nejad *et al.* 2018). A typical result is shown in Figure 5(a), where a 2-mm MN dermaroller was rolled over the gel single time. Since both the dye and the polymer are hydrophilic, dye-coated MNs penetrated and left most of the dye particles into the gelatine gel. Transferred dye completely diffused inside the gelatine gel in 6 h (Figure 5(a)). Clearly, dye-loaded nanoparticles can be delivered into the artificial skin made of gelatine gel.

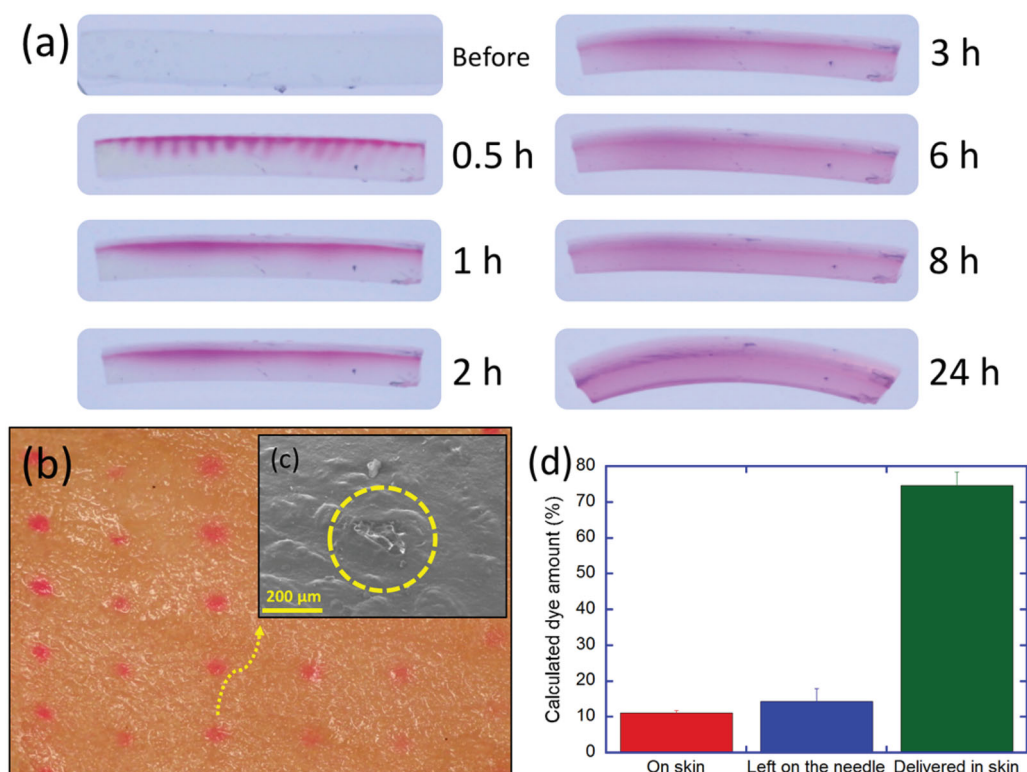


Figure 5. Application of dye-coated MN dermaroller: (a) cross-sectional observation of dye diffusion on gelatin gel; (b) application of dye-coated 2 mm dermaroller on porcine skin; (c) SEM image of porcine skin after application; (d) typical dye percentage breakdown between the amount on skin, retained on the dermaroller (2 mm), and delivered into porcine skin.

Porcine skin is very comparable with human skin and has been used in multiple studies as a model for human skin (Summerfield *et al.* 2015). After the application of the 2 mm MN dermaroller on porcine skin, the MNs exhibited the ability to deliver the dye onto the skin as shown in Figure 5(b). The MNs created small holes on the stratum corneum and released the most of contents inside the skin (Figure 5(c)).

While the MN tip is in intimate contact with the interior of the skin during insertion, the lower parts of the MN close to the dermaroller base have more limited contact. Therefore, less than 100% of the dye can be delivered. On the average $\sim 15\%$ of the dye was retained on the MNs, $\sim 10\%$ of dye was left on the skin surface and more than 70% of dye was delivered inside the skin (Figure 5(d)). For a typical example, a total dye amount for 30 min electrospaying on 2 mm MNs was found to be $\sim 256 \mu\text{g}$, of which $\sim 180 \mu\text{g}$ is delivered into the skin. While dye loading is a function of electrospaying process time, the dye concentration, and the geometry of the MN array, our loading amount and delivery efficiency were found comparable with that obtained by the dip coating method (70–90%) (Ma and Gill 2014). In this study, single pass rolling was found sufficient to reach more than 70% delivery of coated material on MNs. Nguyen *et al.*

(2016) used uncoated dermarollers applied as many as 15 times to disrupt the stratum corneum barrier prior to enhancing TDD. In this study, we can efficiently combine the perforation of the stratum corneum and the application of drug molecules using the electro-spray drug-coated MN array dermarollers.

The effectiveness of our approach was evaluated *in vivo* using a rat model with diabetes. Since dermal thickness of rats is reported to be $\sim 2 \text{ mm}$ (Wei *et al.* 2017), two different dermarollers with needle heights of 1 and 2 mm were selected to investigate the effect of MN height on intradermal application. Insulin was successfully coated on both 1 and 2 mm MNs using the electrospaying method. It was found that blood glucose levels increased in most animals during the first hour (Figure 6). This could be caused by stress due to the shaving process or by MN insertion on the dorsal region of the skin. After the first hour, blood glucose levels started to decrease for both MN heights. The decrement was more evident for the 2 mm MN for 1–4 h. Although a slight increase of blood glucose levels was observed for 1 mm MN group after 4 h, MN groups maintained consistent glucose level at around 80%. Similar to our results Economidou *et al.* (2019) reported that insulin coated 3D MNs maintained the blood glucose at steady state

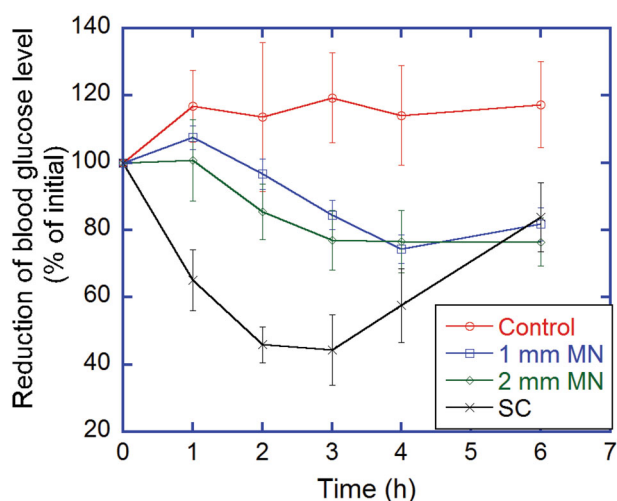


Figure 6. Comparison of blood glucose levels between control, 1 mm MN, 2 mm MN and subcutaneous (SC) insulin groups (mean \pm SE) ($n = 6$).

level up to 4 h. As expected, subcutaneous insulin injection decreased blood glucose levels more rapidly and strongly than insulin coated MNs due to the depth of needle penetration. The difference in blood glucose levels between subcutaneous and MN groups might be due to the difference of delivered insulin concentration into the skin. In Figure 5, ~70% of dye was delivered inside the porcine skin. Therefore, delivered insulin concentration in MN groups will be lower than SC group.

To improve the efficiency of insulin delivery through skin by MN, a higher dose has to be applied to MNs. Interestingly, the blood glucose levels in the SC group increased rapidly after 3 h and were roughly the same as the MN groups at the 6 h period. Furthermore, the glucose level fluctuations observed for the SC group may induce health problems, such as asthma, eczema or joint pain. Insulin delivery using MNs decreased the blood glucose levels in a more consistent manner compared to subcutaneous injection. As shown in Figure 5(a), the transferred dye was visually observed to completely diffuse inside the gelatin gel in ~6 h. Similarly, MN transferred insulin inside the rat skin can be absorbed into the blood stream in a sustained way, leading to a more consistent effect compared to subcutaneous injection. Economidou *et al.* (2019) also stated that the insulin-coated MNs released the insulin transdermally to blood capillaries via passive diffusion.

4. Conclusions

In summary, the electrospaying technique was successfully used for coating of MN dermarollers with

different heights of MNs. Electrospaying is shown to be a very versatile method to coat the metallic MNs. One-time application of 2 mm MN dermaroller was sufficient to reach more than 70% delivery of the material coated on MNs into porcine skin. Our preliminary *in vivo* studies showed that the coated MNs were more successful in maintaining the blood glucose levels steady over 6 h period compared to traditional subcutaneous injection. Microneedles coated with electrospayed nanoparticles can be used in a variety of applications such as painless cosmetic application with hydrating agents (such as hyaluronic acid), drug delivery of anaesthetics (such as lidocaine) or local delivery of nutrients (vitamins such as retinol) and also for systemic delivery of peptide/proteins.

Disclosure statement


No potential conflict of interest was reported by the author(s).

Funding

ST was awarded a scholarship by the Scientific and Technical Research Council of Turkey [TUBITAK-BIDEB 2219].

ORCID

Serdar Tort  <http://orcid.org/0000-0003-4945-5420>

Necibe Basaran Mutlu Agardan  <http://orcid.org/0000-0002-4882-3124>

Daewoo Han  <http://orcid.org/0000-0002-0689-555X>

Andrew J. Steckl  <http://orcid.org/0000-0002-1868-4442>

References

- Alyami, H., *et al.*, 2017. An investigation into the effects of excipient particle size, blending techniques and processing parameters on the homogeneity and content uniformity of a blend containing low-dose model drug. *PLOS one*, 12 (6), e0178772.
- Anderson, J.A., *et al.*, 2016. Preparation, characterization, in vitro drug release, and cellular interactions of tailored paclitaxel releasing polyethylene oxide films for drug-coated balloons. *Acta biomaterialia*, 29, 333–351.
- Apicella, A., *et al.*, 1993. Poly(ethylene oxide) (PEO) and different molecular weight PEO blends monolithic devices for drug release. *Biomaterials*, 14 (2), 83–90.
- Aronson, R., 2012. The role of comfort and discomfort in insulin therapy. *Diabetes technology & therapeutics*, 14 (8), 741–747.
- Baek, S.-H., Shin, J.-H., and Kim, Y.-C., 2017. Drug-coated microneedles for rapid and painless local anesthesia. *Biomedical microdevices*, 19 (1), 2.
- Bass, P., *et al.*, 2018. Enhancement of biodegradable poly(ethylene oxide) ionic-polymer metallic composite

- actuators with nanocrystalline cellulose fillers. *Actuators*, 7 (4), 72.
- Bulboacă, A.E., et al., 2019. Liposomal curcumin is better than curcumin to alleviate complications in experimental diabetic mellitus. *Molecules*, 24 (5), 846.
- Chen, J., et al., 2015. Controllable coating of microneedles for transdermal drug delivery. *Drug development and industrial pharmacy*, 41 (3), 415–422.
- Chen, X., et al., 2009. Dry-coated microprojection array patches for targeted delivery of immunotherapeutics to the skin. *Journal of controlled release*, 139 (3), 212–220.
- Chen, Y., et al., 2017. Fabrication of coated polymer microneedles for transdermal drug delivery. *J Control release*, 265, 14–21.
- Dhawan, S., et al., 2005. Applications of poly(ethylene oxide) in drug delivery systems part II. *Pharmaceutical technology*, 29 (9), 82–96.
- Economidou, S.N., et al., 2019. 3D printed microneedle patches using stereolithography (SLA) for intradermal insulin delivery. *Materials science & engineering C: materials for biological applications*, 102, 743–755.
- Escobar-Chávez, J.J., et al., 2011. Microneedles: a valuable physical enhancer to increase transdermal drug delivery. *Journal of clinical pharmacology*, 51 (7), 964–977.
- Gill, H.S., and Prausnitz, M.R., 2007. Coated microneedles for transdermal delivery. *Journal of controlled release*, 117 (2), 227–237.
- Guo, Q., et al., 2015. Fabrication of polymeric coatings with controlled microtopographies using an electrospaying technique. *PLOS one*, 10 (6), e0129960.
- Gupta, J., Felner, E.I., and Prausnitz, M.R., 2009. Minimally invasive insulin delivery in subjects with type 1 diabetes using hollow microneedles. *Diabetes technology & therapeutics*, 11 (6), 329–337.
- Haj-Ahmad, R., et al., 2015. Microneedle coating techniques for transdermal drug delivery. *Pharmaceutics*, 7 (4), 486–502.
- Hamoudi-Ben Yelles, M.C., et al., 2017. PLGA implants: how poloxamer/PEO addition slows down or accelerates polymer degradation and drug release. *Journal Control Release*, 253, 19–29.
- Han, D., et al., 2017. Stimuli-responsive self-immolative polymer nanofiber membranes formed by coaxial electrospinning. *ACS applied materials & interfaces*, 9 (13), 11858–11865.
- Han, D., and Steckl, A.J., 2017. Selective pH-responsive core-sheath nanofiber membranes for chem/bio/med applications: targeted delivery of functional molecules. *ACS applied materials & interfaces*, 9 (49), 42653–42660.
- Ingrole, R.S.J., and Gill, H.S., 2019. Microneedle coating methods: a review with a perspective. *The journal of pharmacology and experimental therapeutics*, 370 (3), 555–569.
- Iriarte, C., et al., 2017. Review of applications of microneedling in dermatology. *Clinical, cosmetic and investigational dermatology*, 10, 289–298.
- Jaworek, A., 2007. Micro- and nanoparticle production by electrospaying. *Powder technology*, 176 (1), 18–35.
- Jaworek, A., and Sobczyk, A.T., 2008. Electrospaying route to nanotechnology: an overview. *Journal of electrostatics*, 66 (3-4), 197–219.
- Khan, H., et al., 2014. Smart microneedle coatings for controlled delivery and biomedical analysis. *Journal of drug targeting*, 22 (9), 790–795.
- Kim, Y.-C., Park, J.-H., and Prausnitz, M.R., 2012. Microneedles for drug and vaccine delivery. *Advanced drug delivery reviews*, 64 (14), 1547–1568.
- Li, S., Li, W., and Prausnitz, M., 2018. Individually coated microneedles for co-delivery of multiple compounds with different properties. *Drug delivery and translational research*, 8 (5), 1043–1052.
- Ma, Y., and Gill, H.S., 2014. Coating solid dispersions on microneedles via a molten dip-coating method: development and in vitro evaluation for transdermal delivery of a water-insoluble drug. *Journal of pharmaceutical sciences*, 103 (11), 3621–3630.
- McGrath, M.G., et al., 2011. Determination of parameters for successful spray coating of silicon microneedle arrays. *International journal of pharmaceutics*, 415 (1-2), 140–149.
- Nejad, H.R., et al., 2018. Low-cost and cleanroom-free fabrication of microneedles. *Microsystems & nanoengineering*, 4 (1), 17073.
- Nguyen, J., et al., 2016. The influence of solid microneedles on the transdermal delivery of selected antiepileptic drugs. *Pharmaceutics*, 8 (4), 33.
- Pere, C.P.P., et al., 2018. 3D printed microneedles for insulin skin delivery. *International journal of pharmaceutics*, 544 (2), 425–432.
- Peters, E.E., et al., 2012. Erythropoietin-coated ZP-microneedle transdermal system: preclinical formulation, stability, and delivery. *Pharmaceutical research*, 29 (6), 1618–1626.
- Pettis, R.J., et al., 2011. Intradermal microneedle delivery of insulin lispro achieves faster insulin absorption and insulin action than subcutaneous injection. *Diabetes technology & therapeutics*, 13 (4), 435–442.
- Shah, R., et al., 2016. Insulin delivery methods: past, present and future. *International journal of pharmaceutical investigation*, 6 (1), 1–9.
- Shiraishi, K., and Yokoyama, M., 2019. Toxicity and immunogenicity concerns related to PEGylated-micelle carrier systems: a review. *Science and technology of advanced materials*, 20 (1), 324–336.
- Singh, A., and Yadav, S., 2016. Microneedling: advances and widening horizons. *Indian dermatology online journal*, 7 (4), 244–254.
- Summerfield, A., Meurens, F., and Ricklin, M.E., 2015. The immunology of the porcine skin and its value as a model for human skin. *Molecular immunology*, 66 (1), 14–21.
- Ullah, A., Kim, C.M., and Kim, G.M., 2018. Porous polymer coatings on metal microneedles for enhanced drug delivery. *Royal society open science*, 5 (4), 171609.
- Vrdoljak, A., et al., 2012. Coated microneedle arrays for transcutaneous delivery of live virus vaccines. *Journal of controlled release*, 159 (1), 34–42.
- Waghule, T., et al., 2019. Microneedles: a smart approach and increasing potential for transdermal drug delivery system. *Biomedicine & pharmacotherapy*, 109, 1249–1258.

- Wang, C., *et al.*, 2012. Quercetin and allopurinol ameliorate kidney injury in STZ-treated rats with regulation of renal NLRP3 inflammasome activation and lipid accumulation. *PLoS one*, 7 (6), e38285
- Wei, J.C.J., *et al.*, 2017. Allometric scaling of skin thickness, elasticity, viscoelasticity to mass for micro-medical device translation: from mice, rats, rabbits, pigs to humans. *Scientific reports*, 7 (1), 1–16.
- Yilmaz, B., and Kadioglu, Y., 2012. Determination of human insulin in pharmaceutical preparation by zero, first and second order derivative spectrophotometric methods. *International research journal of pharmaceutics*, 2 (2), 21–29.
- Yu, D.-G., *et al.*, 2011. Polymer-based nanoparticulate solid dispersions prepared by a modified electrospraying process. *Journal of biomedical science and engineering*, 04 (12), 741–749.